

Space-Time Decoupled Information Metasurface

Xuehui Dong^{1,*}, Miyu Feng¹, Bokai Lai¹, Chen Shao¹, Tiebin Mi^{1,*}, and Robert Caiming Qiu^{1,*}

¹School of Electronic Information and Communications, Huazhong University of Science and Technology, Wuhan, 430074, China

*Corresponding author: {xuehuidong, mitiebin, caiming}@hust.edu.cn

ABSTRACT

Information metasurface is a type of metasurface device capable of rapidly altering its EM characteristics to generate specific information. Past research presents various strategies for embedding information into ambient EM waves through the superposition of each unit's quantified properties. Despite their capabilities, these approaches alone are insufficient for independently managing the creation of information and the allocation of spatial energy. Here, we propose a general theory of space-time decoupled metasurface (STD-Metasurface) to obtain the completely independent manipulation of information generating and spatial filtering. As proof-of-concept demonstration, we design a single-diode small-signal-modulation based prototype, capable of generating precise arbitrary waveforms while maintaining unaltered beam patterns. We exhibit how the superiority of the STD-Metasurface enhance its practicality and facilitate its application as a reconfigurable backscatter transmitter and an dynamic Doppler-spoofing reflection tag.

Introduction

The essence of information is defined as the variations in objects relative to a subject. In wireless electromagnetic (EM) systems (such as wireless communications and radar), EM waves serve as the primary medium for information transmission. The information is embedded in the variations carried by the waves, whereas their spatial distribution or propagation path constitutes the information channel, also known as the communication channel. Recently, metasurface, comprised of 2D arrays of sub-wavelength reconfigurable units, has attracted great attention due to their simple structures without radio frequency (RF) components and their remarkable capabilities in manipulating EM wave and even producing information.

With the advancement of EM metamaterials, a new technology has emerged that generates information based on EM metasurfaces, referred to as information metasurfaces. In 1898, J.C. Bose first discovered that a helical coil could alter the polarization direction of EM waves, marking the beginning of human understanding that artificial materials could modify the properties of EM waves¹. In 1952, Schelkunoff and Friis identified that artificial materials exhibited artificial magnetism, a property not found in nature². In 1999, Rodger Walser introduced the term "metamaterials" at a DARPA symposium, describing them as materials capable of entirely novel responses not seen in the natural world³. In 2003, Sievenpiper and colleagues first proposed the concept and prototype of reconfigurable metasurfaces, stating that "the periodic surface impedance distribution can alter the surface's EM characteristics"⁴. In 2014, Cui and his team in China introduced the concept and prototype of digital-coding metasurfaces, 'bridging the physical and digital worlds'⁵. Using field-programmable array devices to dynamically adjust the EM characteristics of the metasurface, they significantly enhanced the reconfigurability and real-time control of EM wave manipulation. In 2017, Cui et al. proposed the concept of information metasurfaces, where the rapid, periodic switching of preset EM characteristic distributions allows these surfaces to "not only control EM waves, but also generate information"⁶. Since then, EM metasurfaces have entered the era of information metasurfaces.

Recent research on how to generate information using metasurfaces can be categorized into three main methods: 1) spatial coding, 2) temporal coding, and 3) space-time coding. Spatial coding involves designing the EM response of metasurface units in a 2D distribution, altering the radiation characteristics of EM waves, and encoding information in the spatial domain. The receiver extracts the information through spatial sampling. This method has been applied to areas such as spatial energy distribution⁵ (beamforming), spatial phase distribution⁷ (holographic imaging), spatial polarization distribution^{8,9}, etc. However, its limitation is that it remains fixed in the time domain. Temporal coding addresses this issue by introducing periodically varying digital control signals that encode information in the time or frequency domains, generating specific time-frequency information. This approach has been utilized for independent control of harmonic amplitude and phase¹⁰, efficient frequency conversion¹¹, multi-polarization conversion¹², etc. In contrast, its drawback lies in the inability to simultaneously control the spatial distribution of EM waves. To overcome these limitations, a digital metasurface-based information generation framework known as space-time coding (STC) was proposed^{6,13}. Its principle is the joint design of the time sequences of the 2D EM response distribution, enabling dynamic control over both the spatial and temporal characteristics of the EM waves. This coding scheme allows information and energy to be encoded at specific locations, enhancing the signal-to-noise ratio (SNR) at the receiver and even improving physical layer security.

However, a key feature within the framework of space-time coding is the coupling between time and space. In this framework, the time domain baseband signal is generated by sequentially switching a predesigned beam sequence,

where each beam is meticulously crafted based on the position of the receiver. The time domain signal depends on the spatial sampling points, meaning that the normalized $E_{\text{scatter}}(\tau; \mathbf{r}_1)$ and $E_{\text{scatter}}(\tau; \mathbf{r}_2)$ exhibit different temporal variations. Although space-time coupling can offer advantages in specific applications, it also imposes significant limitations on the broader applicability of information metasurfaces, leading to three key challenges that are difficult to address:

- **Precise generation of arbitrary signal:** The discretization of EM characteristics and control signal make it difficult to generate continuous arbitrary waveforms and spectra;
- **Complex spatial environments:** When the signal is encoded at specific spatial locations, changes or uncertainties in the environment hinder accurate transmission;
- **Beam variation pattern leakage:** Signal generation relies on changes in spatial distribution, making variation patterns in the side lobes susceptible to interception and detection.

The challenges in addressing the three aforementioned issues stem from the following: (1) a lack of continuous signal control over metasurface units, preventing the generation of continuous electromagnetic properties; (2) the inability to truly modulate the baseband signal onto a radio frequency (RF) carrier, instead relying on the superposition principle to control the amplitude and phase parameters of the electromagnetic field at specific spatial sampling points; (3) The failure to decouple the variations in the spatial domain from those in the time domain.

Fundamentally, this coupling effect arises from insufficient degrees of freedom to control the electromagnetic characteristics of each individual unit. To eliminate this coupling effect, we aim to achieve:

$$E_{\text{scatter}}(\tau, \mathbf{r}) = \tilde{E}_{\text{scatter}}(\tau) \bar{E}_{\text{scatter}}(\mathbf{r}), \quad (1)$$

where $\tilde{E}_{\text{scatter}}(\tau)$ and $\bar{E}_{\text{scatter}}(\mathbf{r})$ represent the temporal and spatial components of the scattered electric field of the

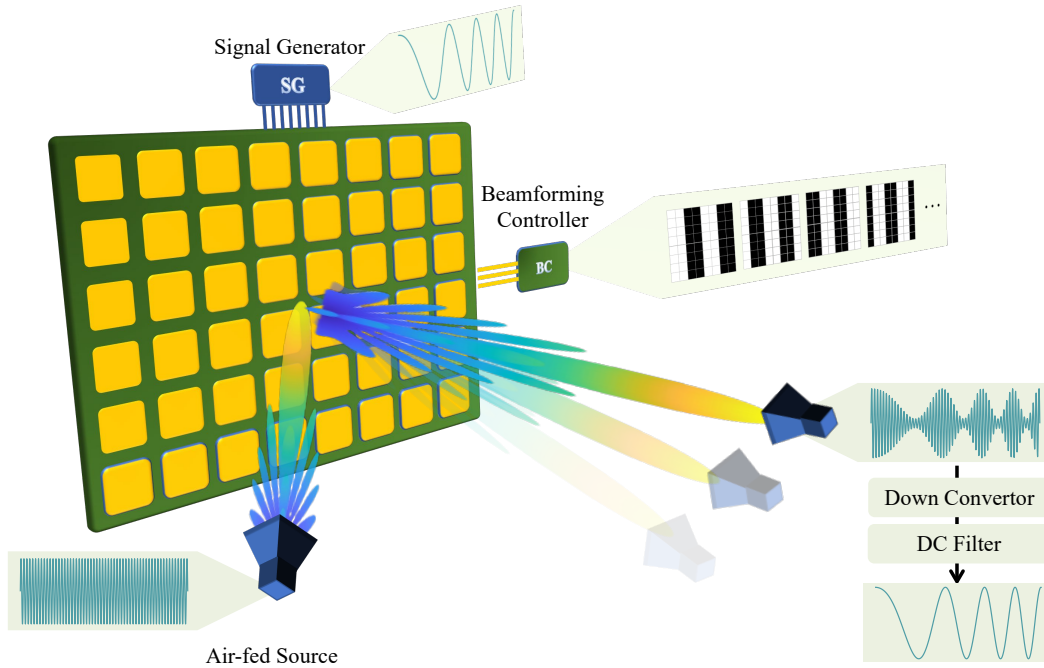


Figure 1. Conceptual illustration of decoupling of scattering EM waves in terms of space and time domain base on STD-Metasurface. By independently controlling the modulation factor and the beam pattern factor of each unit, the sampling in time domain represents the information modulated by STD-Metasurface, and spatial energy distribution in space domain. Here we illustrate that the signal generator modulate the continuous baseband signal onto the air-fed source, meanwhile the varying discrete codebook sequence aligns the main-lobe of the beam to the moving receiver.

metasurface, respectively. The former carries the information varying over time, while the latter manages the spatial energy distribution. Fortunately, this functional separation aligns with the logic of traditional multi-antenna transmitters. In RF links, a mixer shifts the spectrum of the baseband signal produced by a digital-to-analog converter (DAC) to near the carrier frequency, and then a phase shifter adjusts the beam direction.

In this work, we propose for the first time the concept of a space-time decoupled metasurface (STD-Metasurface), where the spatial properties $\tilde{E}_{\text{scatter}}(\tau)$ and temporal properties $\bar{E}_{\text{scatter}}(r)$ of the scattered electric field can be independently controlled. We also designed and fabricated a space-time decoupled metasurface based on small-signal modulation using a

single diode, where each unit cell employs just one PIN diode to independently achieve both beamforming and continuous signal modulation. This allows for the generation of arbitrary waveforms and spectra while maintaining a fixed spatial energy distribution.

At the application level, we built a prototype system based on the STD-Metasurface. By utilizing beamforming and designing arbitrary symbol waveforms, the system adapts to complex channels, enhancing the signal-to-noise ratio (SNR) after matched filtering at the receiver. This enables backscatter communication with passive beamforming functionality. Additionally, as a scatterer radar tag, the system can control the spatial energy distribution to reduce radar cross-section (RCS), and it can generate arbitrary micro-Doppler signatures with low interception probability.

Results

Theory of Space-Time Decoupled Metasurface

Here we illustrate the fundamental concept of space-time decoupling, and model the STD-Metasurface as a space-time transfer function (STTF) which consists of two parts signal modulator and spatial filter. First, we recall that the Eq.(1) divides the equation into two parts: 1) time-varying part, carrying responsible for the information, and 2) space-varying part, managing the spatial energy distribution. According to the array signal processing theory¹⁴, the spatial distribution is the 2D discrete Fourier transform (DFT) of the phase distribution of the surface. So that we consider a time-varying general reflection coefficients (GRC) of n th unit as

$$\Gamma_n(\tau, t) = \gamma_n(\tau) e^{j\theta_n(t)} \quad (2)$$

where τ and t respectively denote the variables in fast-time domain and slow-time domain. The fast time-domain component $\gamma_n(\tau) \in \mathbb{C}$ is referred to as the modulation factor. The slow time-domain part $e^{j\theta_n(t)}$ determines the phase difference between the emitted and incident waves and is known as the beam pattern factor.

The fast-time domain part of GRC is defined as the variation of the states between the emitted and incident waves. This can refer to various electromagnetic parameters that the metasurface can rapidly adjust, such as amplitude^{15,16}, phase^{17,18}, amplitude and phase combined¹⁹, or even polarization direction²⁰, orbital angular momentum^{21,22}, and so on. Here we define two important vectors, EM characteristic vector $\varepsilon(\tau, t)$ and reflective array manifold vector $\mathbf{v}(\mathbf{k}_r, \mathbf{k}_i; \mathbf{P})$ (see Supplementary.A). The former one represents all the programmable EM characteristics, and the latter decides the size and shape of STD-metasurface. where \mathbf{k}_r and \mathbf{k}_i denotes the wavenumber vectors of outgoing and incident waves. The columns of \mathbf{P} denotes the coordinates of the center of each unit. Given the coordinate matrix \mathbf{P} , we can obtain the STTF of STD-metasurface by

$$\mathcal{T}_{STD}(\tau, t, \mathbf{k}_r, \mathbf{k}_i) = \varepsilon^T(\tau, t) \mathbf{v}(\mathbf{k}_r, \mathbf{k}_i). \quad (3)$$

Without loss of generalization, ignoring the spatial wideband effects and path loss, the relationship between the reflected field and incident field (see Supplementary.A for details), during one slow-time scaling, can be expressed as

$$E_r(\tau, \mathbf{k}_r; \{\gamma_n(\tau)\}, \{\theta_n\}) = \underbrace{\tilde{E}_r(\tau) \tilde{E}_r(\mathbf{k}_r)}_{\text{signal modulator}} = \underbrace{\tilde{E}_i(\tau) \sum_{n=0}^{N-1} \gamma_n(\tau) \cdot \iint d\mathbf{k}_i \cdot \mathbf{w}^T \mathbf{v}(\mathbf{k}_r, \mathbf{k}_i) \tilde{E}_i(\mathbf{k}_i)}_{\text{spatial filter}}. \quad (4)$$

where $\mathbf{w} = [e^{j\theta_0}, e^{j\theta_1}, \dots, e^{j\theta_{N-1}}]^T$. The Eq.(4) reflects the form of space-time decoupling that we aimed to present in Eq.(1), as long as the modulation factor and beam pattern factor can be independently controlled. This allows for the separate manipulation of the time-domain and space-domain characteristics, thereby achieving the desired decoupling. For convenience, we express the spatial domain in the discretized angular domain and only consider the propagation of electromagnetic waves in the yOx plane. Assuming the fast-time variations of the incident waves from all directions are identical, i.e., $\mathbf{E}_i(\tau) = \tilde{E}_i(\tau) \mathbf{E}_i$, then we obtain

$$\mathbf{E}_r(\tau) = \tilde{E}_r(\tau) \mathbf{E}_r = \gamma_{\text{total}}(\tau) \tilde{E}_i(\tau) \mathbf{T}_{STD} \mathbf{E}_i \quad (5)$$

The equation has been expressed in two distinct parts, signal modulator $\tilde{E}_i(\tau) = \gamma_{\text{total}}(\tau) \tilde{E}_i(\tau)$ and spatial filter $\mathbf{E}_r = \mathbf{T}_{STD} \mathbf{E}_i$, where the spatial filter matrix $\mathbf{T}_{STD} = \{\mathbf{w}^T \mathbf{v}(\mathbf{k}_p, \mathbf{k}_q)\}_{pq}$.

The general framework of STD-Metasurface has already established in Eq.(4) and Eq.(5). It is easy to find that the information carried by the outgoing wave is entirely determined by the modulation factor of each element in the fast time domain, while the energy distribution of the outgoing wave is fully dependent on the beam pattern factor of each element in the slow time domain.

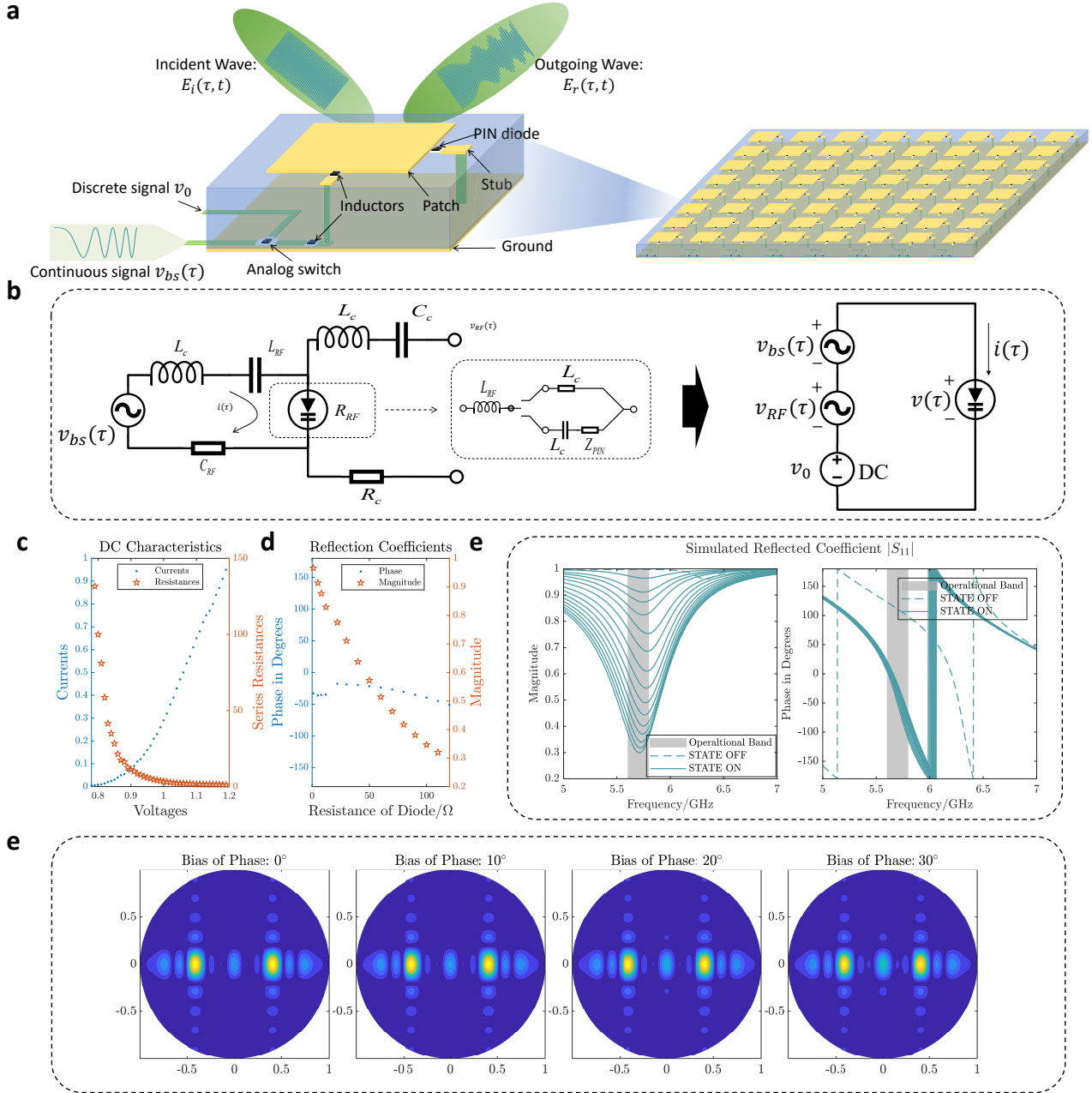


Figure 2. Hardware design of single-diode small-signal-modulation magnitude-phase decoupled unit. **a.** Schematic of the unit design. Combining the continuous signal $v_{bs}(\tau)$ and the discrete signal v_0 by applying the CMOS transistor based analog switch. By applying the inductors, the high-order cross-terms in Eq.(6) are filtered out and RF incident waves are choked from control circuits. **b.** The equivalent circuits of proposed unit (left) can be simplified as a single-diode mixer circuit. **c.** The measured DC characteristics of *SMP1345_079LF* is nonlinear as the voltage increasing when it is forward-conducting. **d.** The magnitude and phase response of unit when the equivalent resistance of diode alters from 0Ω to 120Ω . **e.** The 1D simulation of unit resulting from CST, where the magnitude dramatically change and the phase barely change as the unit is at state ON. **f.** The beam pattern barely changes under the phase jitter less than 30° when the quantification of phase is 1-bit.

Single-diode Small-signal-modulation based STD-Metasurface

Based on the aforementioned theoretical framework, we need to redesign the metasurface to increase the degrees of freedom in controlling the EM characteristics of the units, enabling a hardware design that can independently control the modulation factor and the phase factor. In a traditional transmitter architecture, mixers are typically used to shift the spectrum from baseband to radio frequency (RF) signals, which, in the time domain, corresponds to the control of the carrier amplitude. Therefore, we define the modulation factor as the amplitude of the narrow-sense reflection coefficient, and the phase factor as its phase.

Our design philosophy focuses on higher efficiency, greater flexibility, lower cost, and reduced power consumption. Thus, we avoid complex structural designs and achieve independent beamforming and continuous signal modulation using only a single PIN diode (or a Schottky diode with lower junction capacitance for generating higher-frequency signals). The unit structure is shown in Fig. 2(a). Next, we will elaborate on the design concept from the perspective of small-signal mixers and the decoupling of the amplitude and phase of the element reflection coefficient.

Single-diode mixer

The equivalent circuit on the left side of Fig. 2(b) depicts our unit design, while the right side shows the simplified equivalent circuit of the single-diode mixer. When the diode is conducting, it can be modeled as a nonlinear resistor, with its small-signal relationship expressed through a Taylor expansion as follows:

$$\begin{aligned} i(\tau) &= I_s \left(e^{\alpha(v_0 + v_{RF}(\tau) + v_{bs}(\tau))} - 1 \right) \\ &\approx I_0 + \frac{v_{RF}(\tau) + v_{bs}(\tau)}{R_d} + \frac{(v_{RF}(\tau) + v_{bs}(\tau))^2}{2R_d'} \end{aligned} \quad (6)$$

where R_d and R_d' respectively denotes the dynamic junction resistance and its first-order derivative. After DC filter and spectrum filters, we can obtain

$$i_{ac}(\tau) \approx \frac{v_{RF}(\tau)v_{bs}(\tau)}{R_d'}. \quad (7)$$

There are two message that Eq.(7) delivers: first, due to the nonlinearity of the diode's junction resistance, two superimposed input voltage signals driving the diode can result in the multiplication of these two voltage signals. The conclusion is that by utilizing the dynamic junction resistance characteristics of the forward-biased PIN (or Schottky) diodes on the metasurface, small voltage signals can be modulated onto the outgoing electromagnetic waves. Secondly, to avoid signal distortion, we need to select a working range where R_d' remains close to a constant. Observing the left plot in Fig. 2(c) (measured DC characteristics of the *SMP1345_079LF* diode), it can be seen that when the voltage across the diode is between 0.76V and 0.82V, the junction resistance remains relatively stable, ensuring undistorted modulation signals. This information helps in setting an appropriate DC bias voltage v_0 when designing the unit cells.

Additionally, when the frequency of the modulated small signal is sufficiently high, parasitic inductance L_p will introduce impedance, hindering performance. Therefore, if the goal is to design an STD-Metasurface capable of high-frequency information transmission, a Schottky diode, which is more suitable for high-frequency mixing, should be used. Furthermore, the parameters of the equivalent RLC control circuit must be optimized for improved performance.

Magnitude-phase decoupled patch

In the previous section, we explained the feasibility and principles of modulating the desired baseband signal onto the envelope of an incident electromagnetic wave without distortion, using small-signal mixers integrated into patch elements with PIN (or Schottky) diodes. Now, we will discuss the design of patch elements and control circuits that can independently control the modulation factor (the amplitude of the reflection coefficient) and the phase factor (the phase of the reflection coefficient) from the perspective of metasurface unit design.

Based on our prior analysis, we identified the requirements for realizing a prototype of space-time decoupled metasurfaces: using continuous signals to control the continuous variation of the reflection coefficient's amplitude and using discrete signals to control corresponding discrete phase shifts. To meet the objectives of low cost and low power consumption, we opted to use only one diode as the sole dynamic component in each unit. As such, only forward-biased units will provide modulation functionality, while zero-biased units will produce a phase difference distinct from forward-biased ones.

As shown in Fig.2(a), we introduced an analog switch composed of CMOS transistors. The discrete signal v_0 controls the switch's on/off state, and the continuous signal's input is limited to a specific range to ensure signal integrity. Fig.2(d) presents the 1D simulation results of our unit design in CST. It can be observed that, under forward bias, the reflection amplitude varies between 0.3 and 0.97 as the equivalent resistance of the diode changes, while the phase remains nearly constant (with only about 15° of fluctuation). For 1-bit phase quantization, this deviation has minimal impact on beamforming, as illustrated in Fig.2(e).

Based on the discussion in the previous section regarding the operating range where the first derivative of the diode's dynamic resistance remains nearly constant, along with circuit measurements, the small-signal input voltage range has been determined to be 500 mV to 610 mV. Each unit element has an average power consumption of less than 8 mW, with the reflection coefficient amplitude varying between 0.8 and 0.3. This results in an effective modulation efficiency of approximately 65%.

Precise Generation of Arbitrary Signal

With the aid of decoupling between time and space, we can easily obtain precise waveform, spectrum and spectrogram without complicated computation and the variation of beam pattern. For the sake of convenient, we set that the incident EM waves only comes from one direction \mathbf{k}_0 (i.e., $\vec{E}_i(\mathbf{k}_i) = 0, \forall \mathbf{k}_i \neq \mathbf{k}_0$) and has constant envelope (i.e., $\vec{E}_i(\tau) = 1$). The reflected EM field can be expressed as

$$E_r(\tau, \mathbf{k}_r) = \gamma_{\text{total}}(\tau) e^{j\omega_c \tau} \cdot \mathbf{w}^T \mathbf{v}(\mathbf{k}_r, \mathbf{k}_0), \quad (8)$$

where $\gamma_{\text{sum}}(\tau)$ represents the sum of envelopes of each reflected waves that satisfies the superposition principle.

Previous works about information metasurface have investigated many methods on increasing the flexibility of information metasurface to generate desired signal. However, these methods rely on the inherent constraints of space-time coupling, whereby the signal is not modulated into the re-radiated EM wave. Instead, it is encoded at specific angle using uniquely organized sequences of codebook. Based on Eq.(8), we can easily generate arbitrary baseband waveform by directly designing the continuous controlling signal, which is produced by an additional digital-analog-converter (DAC) (see Fig.6). We set a series of experiments to demonstrate the flexibility (see Fig.3).

First, we verified that the STD-Metasurface can generate several classic waveforms, as shown in Fig.3(a). Next, we validated the superposition principle derived from Maxwell's equations, which is fundamental to signal processing theory. We demonstrated multiple combined waveform results under two different inputs. The results in Fig.3(b) show the scaled transmission and convex combination of two classic waveforms (square wave and sine wave). Furthermore, Fig.3(c) displays the spectrum of the received signal generated by the superposition of eight sine signals with arbitrary frequencies and amplitudes. In Fig.3(d), we used a single input to generate a time-frequency spectrum resembling the desired image. Initially, we created the desired image, ensuring its vertical symmetry since a real signal was required. The resolution of the desired image was matched with the sampling rate and number of points in the discrete Fourier transform. The control signal was obtained through an inverse short-time Fourier transform (ISTFT). The input wave was a continuous single-frequency signal, and the received baseband signal consisted of a DC component, noise, and the desired signal. After performing pre-processing steps like noise reduction and DC filtering, we applied a short-time Fourier transform (STFT) to the received time-domain signal to finally obtain the corresponding time-frequency spectrogram.

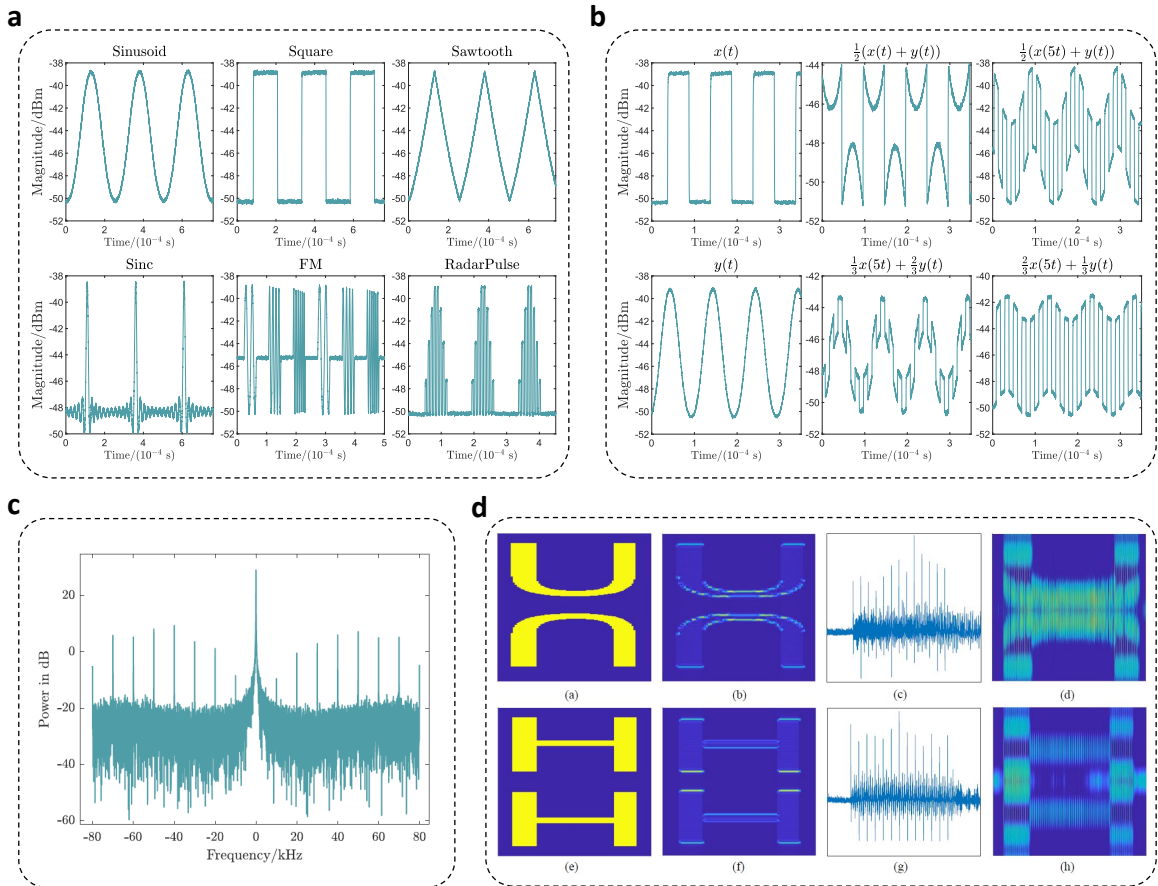


Figure 3. Waveforms or Spectrum generated by STD-Metasurface. a. Several classic waveforms generated by one input. **b.** The convex combination of two scaled waveforms generated by two inputs, which validates superposition principle. **c.** Generating arbitrary spectrum by STD-metasurface. **d.** Spectrogram imaging.

Reconfigurable Backscatter Transmitter

The function of an information metasurface is to embed information into the ambient EM waves, eliminating the need for high-power consumption modules like RF chains and power amplifiers. In the introduction, we provided an overview of current research on how information metasurfaces generate information. In this section, we will delve into how the space-time decoupled metasurface, when used as a wireless communication transmitter, demonstrates greater flexibility and efficiency compared to previous related works.

Firstly, the primary advantage of STD-Metasurfaces over space-time coupled metasurfaces is the ability to modulate arbitrary waveform signals onto the outgoing EM wave without altering the beam pattern. Instead of encoding information at specific positions in the reflection field, as shown in Fig.4, different receivers (RX1 and RX2) in various directions can correctly receive and decode the digital information. This characteristic provides robustness for information transmission in complex or time-varying channels without extremely precise channel state information. Secondly, the capability to generate arbitrary precise waveforms enables the STD-Metasurface transmitter to utilize a variety of advanced modulation techniques. The modulation scheme is reconfigurable, allowing the selection of techniques such as BPSK, AM, FM, and others to increase symbol rates and interference resistance, such as spread spectrum techniques, precoding methods and so on. In Fig.4, the waveform of the symbols is also reconfigurable, allowing dynamic selection of modulation waveforms based on different channel conditions and transmission rate requirements. Moreover, compared to traditional backscatter transmitters, STD-Metasurfaces can control the spatial distribution of the outgoing wave's energy, i.e., beamforming, without disturbing the baseband signal of the EM wave. This significantly enhances the signal-to-noise ratio (SNR) at the receiver. Additionally, it minimizes energy received by eavesdroppers, achieving a degree of physical-layer security. In Fig.4, the eavesdropper receives almost no reflected EM energy, making it impossible to correctly receive the signal or even detect the transmitter's presence.

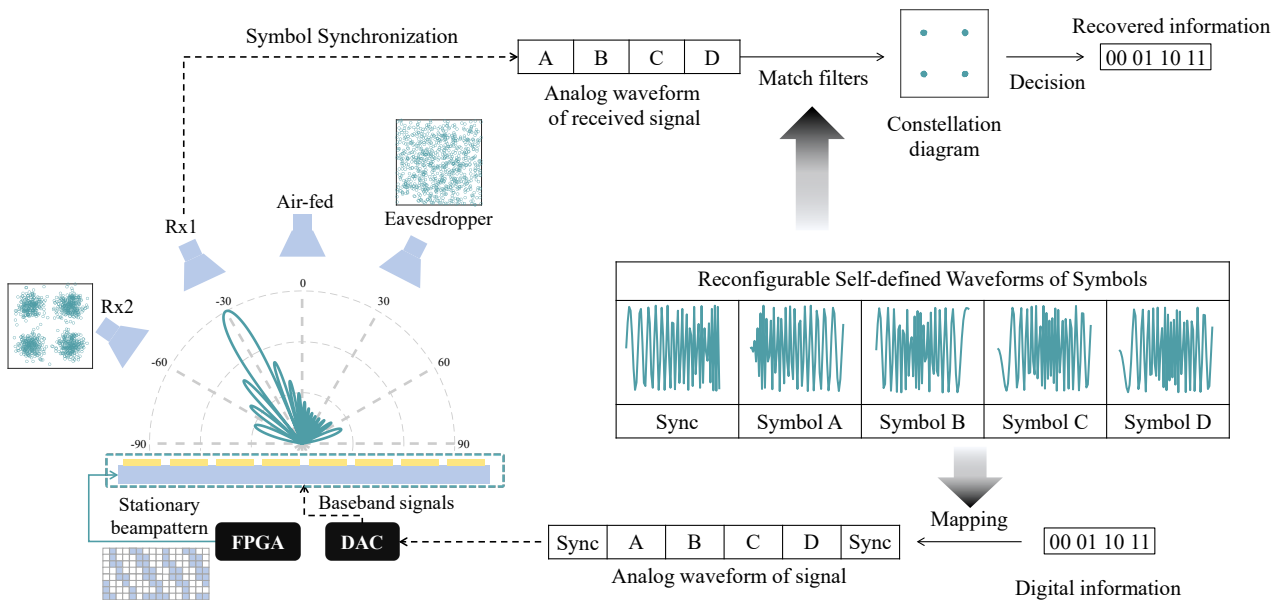


Figure 4. Reconfigurable backscatter transmitter based on STD-Metasurface. The reconfigurability comes from three aspects: 1) modulation technique, 2) waveform of symbols and 3) reflected beam pattern. The main-lobe points to Rx1, while the secondary lobe points to Rx2, so both receive the information correctly. Meanwhile the eavesdropper can not detect the transmission.

Dynamic Doppler-spoofing Reflection Tag

Metamaterials or metasurface devices are often used as radar stealth coatings or deception tags. However, with the advent of information metasurfaces, the flexibility and reconfigurability of metasurfaces as radar deception tags have significantly improved. Existing information metasurfaces, when used as Doppler radar deception reflection tags, face two difficult challenges: (1) Due to space-time coupling, signals differ at various positions, making it easy to detect that the forged signal is artificial; (2) The unknown position of the radar makes it difficult to present the radar with the desired custom waveform. These two major issues greatly limit the practical use of metasurfaces as radar reflection tags.

The introduction of STD-Metasurfaces can address these two problems. As shown in Fig.5, by performing an inverse short-time Fourier transform (ISTFT) on the desired spectrogram, the time-domain waveform can be obtained, and the corresponding range of time-domain voltage waveforms can be input into the STD-Metasurface through a DAC. Since the waveform is modulated in the time domain of the outgoing wave, every point in space can receive the same signal, assuming no noise. In this scenario, the beamforming controller often doesn't need to be active, as there is no specific

target location or task to enhance the echo signal strength. If, in addition to deception, there is a need to reduce the radar cross-section (RCS) of other targets, the function in terms of spatial filter can be controlled by optimizing the codebook. This allows for a significant reduction in the echo signal strength at every radar position. STD-Metasurface makes dynamic radar-spoofing reflection tags more practical and easier to implement.

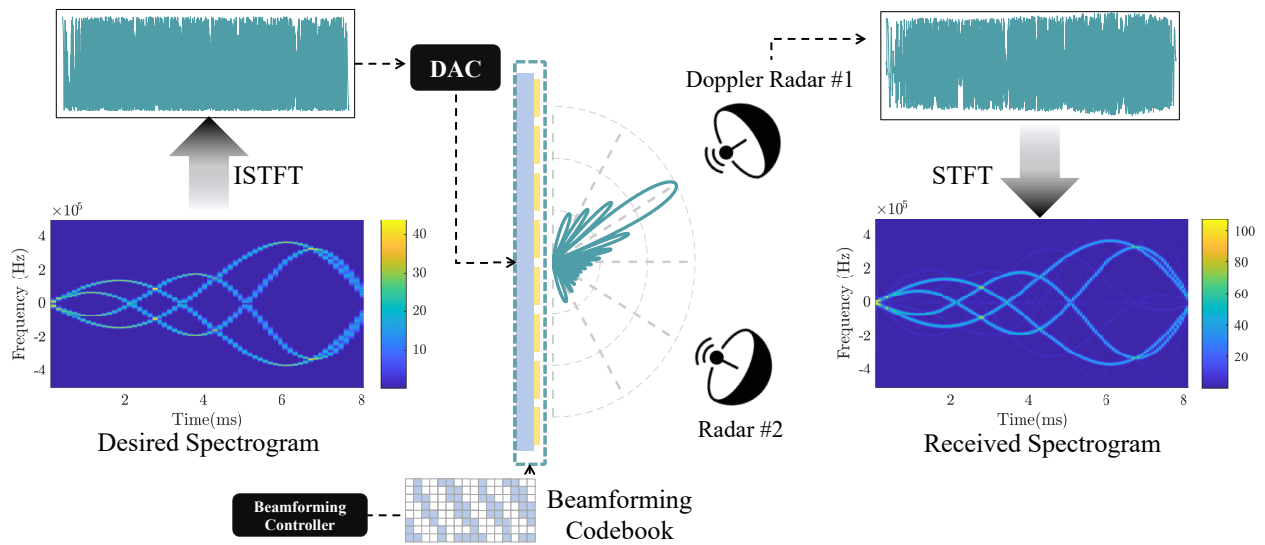


Figure 5. System diagram of the dynamic Doppler-spoofing reflection tag. The desired time-domain waveform is generated based on the specified spectrogram, while spatial energy distribution of the echo can be controlled to deceive target detectors.

Discussion

===conclusion===

Methods

Prototype and Experimental Platform

All the data in the previous sections were collected from the experimental platform as well as the prototype (see Fig.6).

References

1. Bose, J. C. On the rotation of plane of polarisation of electric wave by a twisted structure. *Proc. Royal Soc. Lond.* **63**, 146–152 (1898).
2. Schelkunoff, S. A., Friis, H. T. & Twersky, V. *Antennas: theory and practice* (1953).
3. Walser, R. M. Electromagnetic metamaterials. In *Complex Mediums II: beyond linear isotropic dielectrics*, vol. 4467, 1–15 (SPIE, 2001).
4. Sievenpiper, D. F., Schaffner, J. H., Song, H. J., Loo, R. Y. & Tangonan, G. Two-dimensional beam steering using an electrically tunable impedance surface. *IEEE Transactions on antennas propagation* **51**, 2713–2722 (2003).
5. Cui, T. J., Qi, M. Q., Wan, X., Zhao, J. & Cheng, Q. Coding metamaterials, digital metamaterials and programmable metamaterials. *Light. Sci. Appl.* **3**, e218–e218 (2014).
6. Zhang, L. *et al.* Space-time-coding digital metasurfaces. *Nat. Commun.* **9**, 4334 (2018).
7. Li, L. *et al.* Electromagnetic reprogrammable coding-metasurface holograms. *Nat. communications* **8**, 197 (2017).
8. Kruk, S. *et al.* Invited article: Broadband highly efficient dielectric metadevices for polarization control. *Apl Photonics* **1** (2016).
9. Wang, S. *et al.* Arbitrary polarization conversion dichroism metasurfaces for all-in-one full poincaré sphere polarizers. *Light. Sci. & Appl.* **10**, 24 (2021).
10. Dai, J. Y., Zhao, J., Cheng, Q. & Cui, T. J. Independent control of harmonic amplitudes and phases via a time-domain digital coding metasurface. *Light. Sci. Appl.* **7**, 90 (2018).
11. Dai, J. Y. *et al.* High-efficiency synthesizer for spatial waves based on space-time-coding digital metasurface. *Laser Photonics Rev.* **14**, 1900133 (2020).

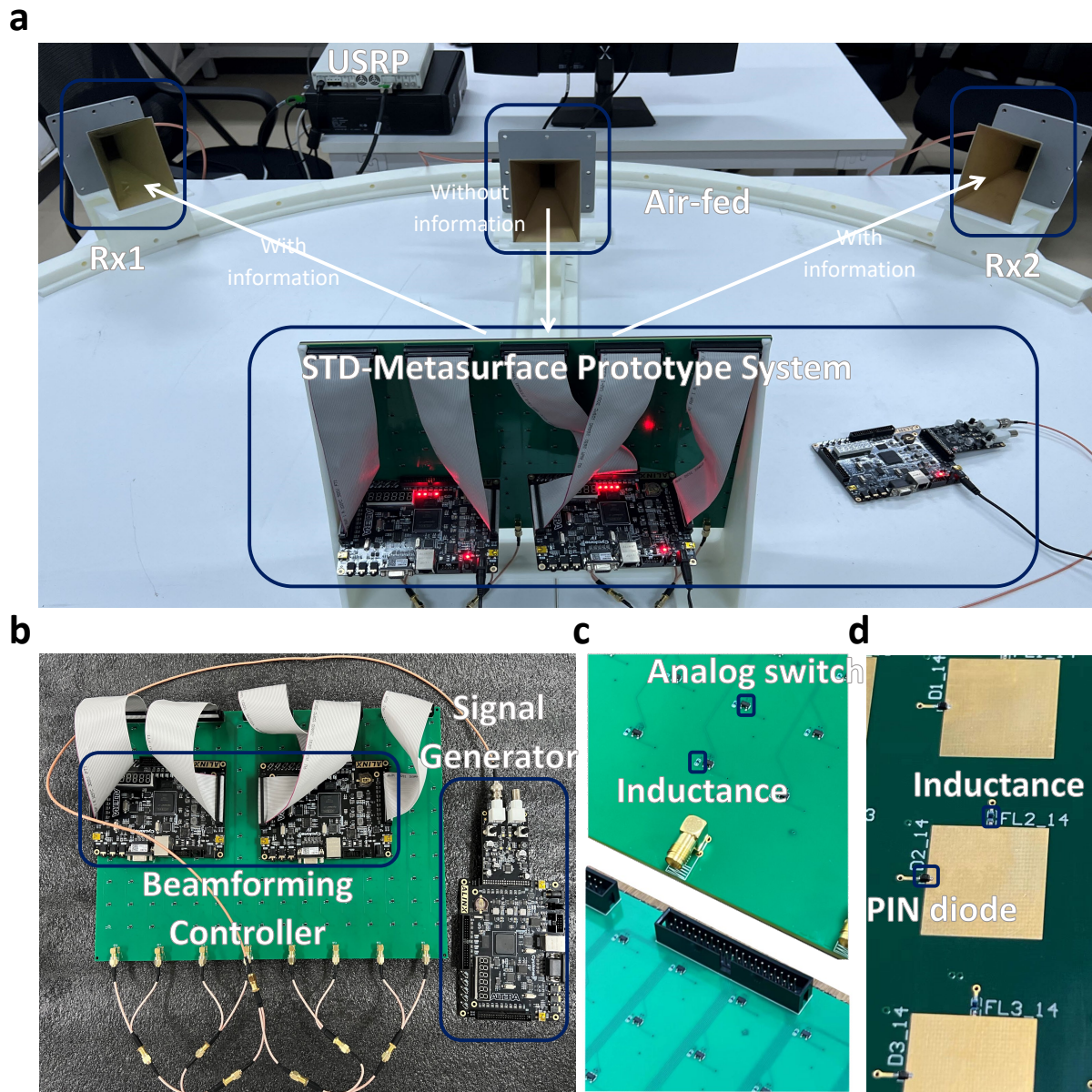


Figure 6. Experimental platform and prototype design.

12. Ke, J. C. *et al.* Linear and nonlinear polarization syntheses and their programmable controls based on anisotropic time-domain digital coding metasurface. *Small Struct.* **2**, 2000060 (2021).
13. Zhang, L. *et al.* A wireless communication scheme based on space-and frequency-division multiplexing using digital metasurfaces. *Nat. electronics* **4**, 218–227 (2021).
14. Van Trees, H. L. *Optimum array processing: Part IV of detection, estimation, and modulation theory* (John Wiley & Sons, 2002).
15. Hong, Q. R. *et al.* Programmable amplitude-coding metasurface with multifrequency modulations. *Adv. Intell. Syst.* **3**, 2000260 (2021).
16. Zhang, Z. *et al.* Active ris vs. passive ris: Which will prevail in 6g? *IEEE Transactions on Commun.* **71**, 1707–1725 (2022).
17. Yang, H. *et al.* A programmable metasurface with dynamic polarization, scattering and focusing control. *Sci. reports* **6**, 1–11 (2016).
18. Kamoda, H., Iwasaki, T., Tsumochi, J., Kuki, T. & Hashimoto, O. 60-ghz electronically reconfigurable large reflectarray using single-bit phase shifters. *IEEE transactions on antennas propagation* **59**, 2524–2531 (2011).
19. Huang, C. *et al.* Graphene-integrated reconfigurable metasurface for independent manipulation of reflection magnitude and phase. *Adv. Opt. Mater.* **9**, 2001950 (2021).

20. Huang, C. X., Zhang, J., Cheng, Q. & Cui, T. J. Polarization modulation for wireless communications based on metasurfaces. *Adv. Funct. Mater.* **31**, 2103379 (2021).
21. Ren, H. *et al.* Metasurface orbital angular momentum holography. *Nat. Commun.* **10**, 2986 (2019).
22. Bai, X. *et al.* High-efficiency transmissive programmable metasurface for multimode oam generation. *Adv. Opt. Mater.* **8**, 2000570 (2020).

Acknowledgements (not compulsory)

Author contributions statement

Additional information

including a supplementary document and three DEMO videos.